Title: Previously reward-associated stimuli capture spatial attention in the absence of changes in the corresponding sensory representations as measured with MEG

Running title: Tracking value-driven attentional capture with MEG

Authors: Tankelevitch L[1,2], Spaak E[1,2,4], Rushworth MFS[1,3], Stokes MG[1,2]

Affiliations:

[1] Department of Experimental Psychology, Wellcome Centre for Integrative Neuroimaging, University of Oxford, Oxford, OX1 3UD, United Kingdom.

[2] Oxford Centre for Human Brain Activity, Wellcome Centre for Integrative Neuroimaging, Department of Psychiatry, University of Oxford, Oxford, OX3 7JX, United Kingdom.

[3] Centre for Functional MRI of the Brain, Wellcome Centre for Integrative Neuroimaging, Nuffield Department of Clinical Neurosciences, John Radcliffe Hospital, University of Oxford, Oxford, OX3 9DU, United Kingdom.

[4] Donders Institute for Brain, Cognition and Behaviour, Radboud University Nijmegen, 6500 HB Nijmegen, The Netherlands

Corresponding author: Mark Stokes, mark.stokes@psy.ox.ac.uk.

Number of pages: 30

Number of figures: 8

Number of words: 234 (Abstract), 773 (Introduction), 1804 (Discussion)

Conflict of interest: The authors declare no competing financial interests.

Acknowledgements:

This research was funded by a Biotechnology and Biological Sciences Research Council (BB/M010732/1) and James S. McDonnell Foundation Scholar Award (220020405) to Mark G. Stokes, and by the NIHR Oxford Health Biomedical Research Centre. The Wellcome Centre for Integrative Neuroimaging is supported by core funding from the Wellcome Trust (203139/Z/16/Z), and The Netherlands Organisation for Scientific Research (NWO Veni grant 016.Veni.198.065 awarded to E.S.).

Abstract

Studies of selective attention typically consider the role of task goals or physical salience, but recent work has shown that attention can also be captured by previously reward-associated stimuli, even when these are no longer relevant (i.e., value-driven attentional capture; VDAC). We used magnetoencephalography (MEG) to investigate how previously reward-associated stimuli are processed, the time-course of reward history effects, and how this relates to the behavioural effects of VDAC. Male and female human participants first completed a reward learning task to establish stimulus-reward associations. Next, we measured attentional capture in a separate task by presenting these stimuli in the absence of reward contingency, and probing their effects on the processing of separate target stimuli presented at different time lags. Using time-resolved multivariate pattern analysis, we found that learned value modulated the spatial selection of previously rewarded stimuli in occipital, inferior temporal, and parietal cortex from ~260ms after stimulus onset. This value modulation was related to the strength of participants' behavioural VDAC effect and persisted into subsequent target processing. Furthermore, we found a spatially invariant value signal from ~340ms. Importantly, learned value did not influence the neural discriminability of the previously rewarded stimuli in visual cortical areas. Our results suggest that VDAC is underpinned by learned value signals which modulate spatial selection throughout posterior visual and parietal cortex. We further suggest that VDAC can occur in the absence of changes in early visual cortical processing.

Significance statement

Attention is our ability to focus on relevant information at the expense of irrelevant information. It can be affected by previously learned but currently irrelevant stimulus-reward associations, a phenomenon termed "value-driven attentional capture" (VDAC). The neural mechanisms underlying VDAC remain unclear. It has been speculated that reward learning induces visual cortical plasticity which modulates early visual processing to capture attention. Although we find that learned value modulates spatial attention in sensory brain areas, an effect which correlates with VDAC, we find no relevant signatures of visual cortical plasticity.

Introduction

Selective attention can be defined as the resolution of competition between stimuli for behavioural control through the enhancement of relevant stimuli and suppression of irrelevant stimuli (Desimone and Duncan, 1995). Traditionally, studies of attention have focused on task demands or physical salience (Beck and Kastner, 2009; Egeth and Yantis, 1997). However, work over recent years has shown that reward history also plays an important role in shaping attention. Stimulus-reward associations continue to capture attention even when they are no longer relevant (Anderson, 2013; Awh et al., 2012; Chelazzi et al., 2013).

Experimentally, value-driven attentional capture (VDAC) is typically established via an initial "training phase" in which visual stimuli are associated with different reward outcomes (e.g., Anderson et al., 2011). During a "testing phase", participants complete a new, formally unrelated task, which re-uses the previously reward-associated stimuli (Anderson et al., 2011). Many studies have shown that these reward-associated stimuli continue to capture attention even in the absence of reward contingency or other task-relevance (Anderson et al., 2011; Raymond and O'Brien, 2009; Theeuwes and Belopolsky, 2012).

Although the phenomenon is well established behaviourally, the neural mechanisms underlying VDAC remain unclear (Anderson, 2016; Chelazzi et al., 2013; Failing and Theeuwes, 2018). Some have suggested that stimulus feature representations in sensory cortex may undergo reward-mediated plasticity during learning (Anderson, 2016; Failing and Theeuwes, 2018; Hickey and Peelen, 2017; van Koningsbruggen et al., 2016). Strengthened representations could then rapidly capture attention in a feed-forward manner, potentially leading to the behavioural effects of VDAC (Anderson, 2016; Failing and Theeuwes, 2018). However, evidence for the existence of this mechanism is limited (Anderson, 2016; van Koningsbruggen et al., 2016).

Electroencephalography (EEG) studies of VDAC show various types of modulations in visual processing (Failing and Theeuwes, 2018). In general, modulations of visual processing can reflect changes in how reward-associated stimuli are processed and/or changes in how *other* stimuli are processed as a result of VDAC (Failing and Theeuwes, 2018). The timing of effects also matters (Luck et al., 2000). Early effects may indicate changes in feed-forward sensory processing of reward-associated stimuli, whereas later effects may reflect attentional modulation triggered by these stimuli (Buffalo et al., 2010; Foxe and Simpson, 2002). Hickey et al. (2010) and Luque et al. (2017) both found an enhanced P1 component for reward-associated stimuli, suggesting modulation of early visual processing of these stimuli. This is consistent with fMRI studies showing that reward-associated stimuli result in increased activation in the ventral visual stream (Anderson et al., 2014; Ghazizadeh et al., 2018). In contrast, Qi et al. (2013) reported that reward-associated stimuli only evoked the later N2pc component, reflecting an attentional shift towards these stimuli. Additionally, others found that reward-associated distracters affected processing of *competing* stimuli, reducing the P1, N1, and N2pc (Itthipuripat et al., 2015; MacLean and Giesbrecht, 2015a).

Comparison between studies is challenging because in some studies the task-relevance, and therefore the reward history, of stimuli changes across trials (e.g., Hickey et al., 2010; Itthipuripat et al., 2015). In other studies, reward-associated stimuli are irrelevant and unrewarded for the entire task (e.g., MacLean and Giesbrecht, 2015; Qi et al., 2013). Furthermore, it is important to isolate effects related to the processing of reward-associated stimuli from those related to the processing of target stimuli (e.g., Hickey and Peelen, 2015).

Finally, it is critical to test whether changes in response amplitude to reward-associated stimuli (as measured using univariate approaches) reflect an improvement in the neural coding of these stimuli (van Ede et al., 2018). For example, Hickey and Peelen (2015) used multivariate pattern analysis (MVPA) to show that fMRI representations of previously reward-associated stimuli are indeed modulated in the ventral visual stream. However, the use of fMRI precludes insight into the timing of these effects during visual processing (Hickey and Peelen, 2015).

In the current study, we used time-resolved MVPA of magnetoencephalography (MEG) data to explore the time-course of cortical representations of previously reward-associated stimuli during VDAC. Participants first completed a reward learning task to establish stimulus-reward associations. We then measured attentional capture in a separate task by presenting these stimuli in the absence of reward contingency, and probing their effects on processing of separate target stimuli. Critically, we also varied the interval between previously reward-associated stimuli and the imperative targets to isolate the neural processes triggered by the reward stimuli, uncontaminated by target processing. Consistent with attentional capture, we found that learned value modulated the spatial selection of previously rewarded stimuli in occipital, inferior temporal, and parietal cortex. However, these effects only emerged from ~260ms after stimulus onset, in contrast to previous evidence of early effects. Moreover, learned value did not modulate cortical representations of the previously reward-associated stimuli.

Materials and methods

Participants

All experiments were conducted under ethical approval from the Central University Research Ethics Committee of the University of Oxford and with informed consent from participants. We aimed for a sample of 30 human participants from the Oxford community for this experiment. Due to poor behavioral performance or MEG acquisition artefacts, we recruited 'replacement' participants as needed, leading to a total sample of 37 participants, aged 19-34 years (M = 24.6 years, SD = 4.2 years; 18 female). All participants were right-handed and had normal or corrected-to-normal vision. One participant was excluded during MEG data acquisition due to inability to follow task instructions, and six participants were excluded prior to data analysis due to artefacts in the MEG data, leaving 30 participants for analysis.

Study structure

Participants completed a *reward learning task* to induce learning of stimulus-reward associations (training phase), and a visual discrimination task (i.e., *attention task)* to test the effect of these associations on visual attention (testing phase). To maximize learning and increase task engagement, participants completed two sessions of each task in an interleaved order on the same day. Participants were compensated based on their winnings in the reward learning task and were explicitly told that the attention task was not rewarded and was simply a requirement to complete as part of the experiment.

Reward learning task (training phase)

The task was presented using MATLAB (MathWorks, MA, USA) and Psychtoolbox-3 (Kleiner et al., 2007). Participants sat 120 cm from the display, which was a Panasonic PT

D7700E (Osaka, Japan) translucent back-projection display, 54.5 × 43cm, resolution 1280 × 1024px, 60 Hz refresh rate. After a 500-1000ms (randomly jittered) inter-trial interval (ITI), two option stimuli (each sized 2.4 × 2.4º visual angle) appeared on screen (Figure 1a). Participants were instructed to maintain fixation until the fixation cross disappeared after 500ms. After the fixation cross offset, participants had 5000ms to indicate their choice with a left or right button press. After the choice, a feedback display presented the outcomes of the chosen and unchosen stimuli. To facilitate learning, the background brightness as well as a presented sound effect indicated the outcome reward magnitude. Participants began the next trial with a button press.

There were 10 option stimuli that participants learned about across trials: two high reward (250 points), two low reward (25 points), and six zero reward stimuli (0 points; Figure 1c). 1000 points were equivalent to £1, with participants receiving their winnings at the end of the experiment. A 'points bar' at the bottom of the screen indicated how many points they had accumulated for the next £1 and a pound (£) counter indicated the total money won thus far. Reward associations were deterministic. To control for possible stimulus difference between option stimuli, reward associations were counterbalanced across participants using a Latin square design. There were 96 High vs. Low reward, 96 High vs. Zero reward, and 192 Low vs. Zero reward choice trials per session, with the latter trial type doubled to equate selection frequency between high and low reward stimuli. Option stimuli varied in both colors and shapes, so participants could use either feature or a combination for learning. Trial order was randomized once and presented consistently across participants to minimize differences in learning.

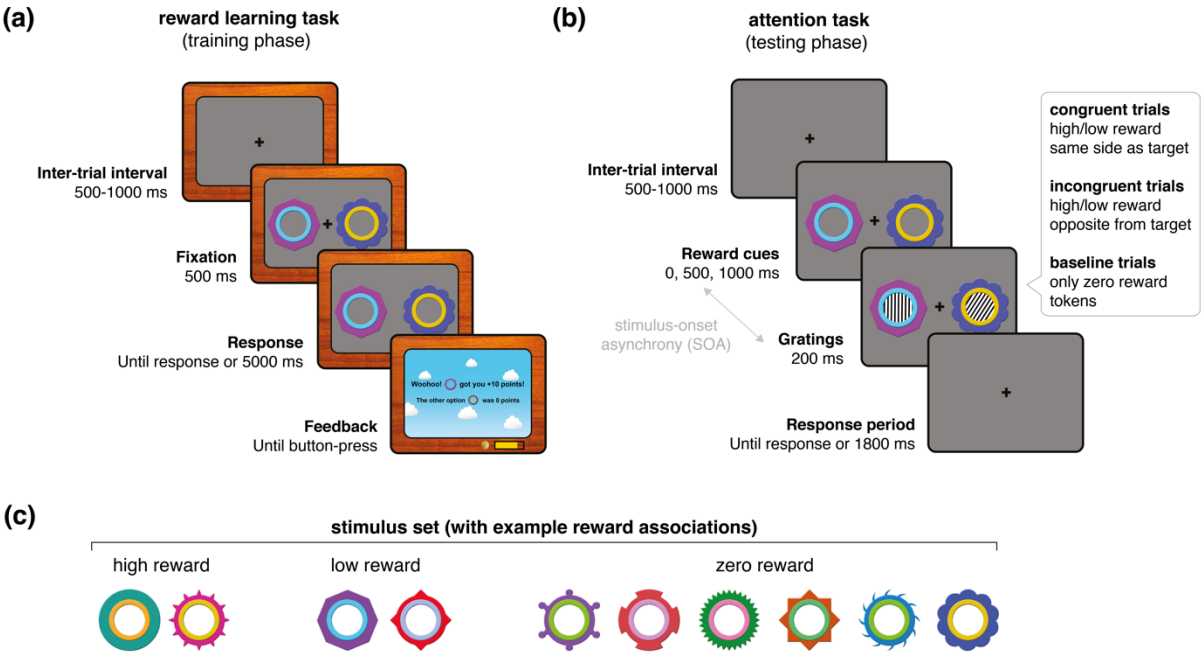

Figure 1. Experimental task design. (a) Experimental design for the reward learning task (training phase). Each trial began with a fixation period (500-1000ms, randomly sampled), followed by the presentation of two option stimuli. After 500ms, the fixation cross disappeared and participants were free to indicate their decision by button-press within the time limit (5000ms). Decisions were followed by a feedback display indicating the points obtained for the chosen stimulus, as well as the points that would have been awarded for the unchosen stimulus. Participants initiated the next trial by button-press. Participants could track their earned points and money with on-screen counters. **(b)** Experimental design for the attention task (testing phase). Each trial began with a fixation period (500-1000ms, randomly sampled), followed by the presentation of two reward stimuli from the previous task (now uninformative and unrewarded). Each trial included one high- or low-reward stimulus together with a zero-reward stimulus, or two zero-reward stimuli (baseline trials). After a stimulus-onset asynchrony (0, 500, or 1000ms), gratings appeared inside the reward stimuli for 200ms. One grating was always either vertically or horizontally oriented (the target), and the other was always oriented obliquely, at one of twelve angles (the distracter). In congruent (incongruent) trials, the target grating appeared on the same (opposite) side as the high- or low-reward stimulus. In trials with two zero-reward stimuli, the target could appear on either side. Reward stimuli and gratings disappeared together after 200ms. Participants had an additional 1800ms to indicate with a button-press whether the target is oriented vertically or horizontally. Note that task stimuli are enlarged for illustration purposes. **(c)** Stimulus set with example associated rewards. Stimulus-reward contingencies were counterbalanced across participants.

Attention task (testing phase)

The hardware and software setup for stimulus presentation was identical to the reward learning task. The task began with a 500-1000ms randomly jittered ITI, during which participants had to fixate on a central cross (Figure 1b). Two of the previously rewarded but currently task-irrelevant reward stimuli then appeared on screen. These could be a pair of High and Zero reward stimuli *(high reward trials)*, Low and Zero reward stimuli (*low reward trials*), or two Zero reward stimuli (*baseline trials*). Following a randomly selected delay of 0, 500, or 1000ms (the *stimulus-onset asynchrony, SOA*), two task-relevant oriented gratings (diameter 1.2º visual angle, with the inner edge positioned 5.4º away from center) appeared inside each of the reward stimuli. The target grating was oriented either 0º or 90º. The participants' task was to indicate this orientation with a button-press. The non-target (distracter) grating was oriented obliquely at 20-70º or 110-160º degrees, randomly selected

from 10º bins. Gratings were presented for 200ms, after which they offset together with the reward stimuli. Participants had up to 1800ms after grating offset to make their response. Auditory feedback was provided with a high frequency tone signifying correct trials and a low frequency tone signifying incorrect trials.

Critically, in high and low reward trials, the target grating appeared inside either the High or Low reward stimuli (*congruent trials*), or inside the Zero reward stimulus (*incongruent trials*). In baseline trials, the target grating could appear in either Zero reward stimulus. Reward stimuli and target locations varied randomly between left and right of the fixation cross.

In each session, there were 60 trials per cell in the reward (3) × congruency (2) × SOA (3) condition matrix, with the exception of the baseline condition in which congruency was not a factor. There were 1800 trials in total across both sessions. All trials were fully randomized across participants. Each session was divided into 19 blocks, with 50 trials per block, and each block taking ~2 minutes to complete. Participants were instructed to maintain fixation and minimize blinking throughout the duration of a block but were able to take a short break after each block.

MEG data acquisition and preprocessing

For both tasks, whole-head MEG data was recorded in a magnetically shielded room using a 306-channel Elekta Neuromag VectorView scanner (102 magnetometers, 204 gradiometers; Elekta, Stockholm, Sweden) at the Oxford Centre for Human Brain Activity (OHBA). Four head position indicator (HPI) coils were placed behind the ears and on top of the forehead to track head movements in the scanner. A magnetic Polhemus Fastrak 3D digitiser pen (Vermont, USA) was used to register the HPI coils and three anatomical landmarks (nasion, left and right auricular points), and digitise the head shape by marking 300 points along the scalp. MEG data were sampled at 1000 Hz with a 0.03-330 Hz bandpass filter during signal digitisation. Electrocardiography (ECG) and electrooculography (EOG) were recorded using electrodes over the wrists and around the eyes (vertical and horizontal for blinks and saccades), and a forehead ground electrode. Eye movements were also recorded using an EyeLink 1000 infrared eye-tracker (SR Research, ON, Canada). Manual responses were collected using a four-button fibre-optic response box.

MEG data were preprocessed using the OHBA Software Library (OSL; ohba-analysis.github.io) and Fieldtrip (Oostenveld et al., 2011). Continuous MEG data were visually inspected to exclude segments containing severe artefacts (e.g., jumps) and interpolate channels that contained frequent severe artefacts. Elekta's Maxfilter Signal Space Separation algorithm was then applied, together with head movement compensation based on the HPI coil data. Due to a stimulus trigger artefact in some participants, timepoints in the data corresponding to stimulus triggers were linearly interpolated within a 15ms window around trigger onset; to be consistent, this correction was done in all participants. Data were then band-pass filtered at 0.1-40 Hz, downsampled to 250 Hz, and epoched from -2000ms to 2000ms relative to grating onset. Eye-blink- and cardiac- related variance was removed by performing Independent Component Analysis (ICA) on the MEG data using the FastICA algorithm and removing any components significantly correlated (using $\alpha = .05$) with vertical EOG and ECG time-courses above a threshold of Pearson's $r = 0.1$. Horizontal EOG, EyeLink, and MEG data were then visually inspected to reject trials containing saccades or other muscle artefacts.

Magnetic Resonance Imaging (MRI) data acquisition

To create subject-specific forward models for MEG source reconstruction, existing structural 3T MRI scans for 16 participants were obtained from previous studies in accordance with data sharing procedures. In addition, new structural MRI scans were acquired for 19 participants on a separate day at the Oxford Centre for Functional MRI of the Brain (FMRIB) using a Siemens Magnetom Prisma 3T scanner, with a T1-weighted MP-RAGE sequence (1×1×1mm isotropic voxels, 256×234×192 grid, echo time = 3.94ms, inversion time = 912ms, recovery time = 1900ms). For this data, participants' noses were included in the field of view to improve registration with the Polhemus head shape and MEG coordinates. MRI data from two participants were not acquired due to early study exclusion and a scheduling issue, respectively. For the latter participant, an average, age-matched (20-24-year-old) brain template was used instead (Richards et al., 2016).

Behavioural data analysis

Behavioural data were analyzed in MATLAB and in R using RStudio (RStudio Inc., Boston, MA, USA) with the *ez* package (Lawrence, 2016). Accuracy in the reward learning task (Figure 2a) was quantified as percent of choices of the higher reward option and in the attention task as percent of correct target-discrimination responses. Reaction time (RT) analyses (Figure 2b) were performed only on correct trials and using the median as the subject-level summary statistic. Behavioral data were analyzed using repeated-measures analysis of variance (ANOVA), followed by pairwise comparisons. Tests were corrected for multiple comparisons using the Holm-Bonferroni method where relevant. Learning curves of accuracy and RT in the reward learning task were computed by smoothing each participant's trial-wise data with a 10-trial moving average window within each session and concatenating sessions. Curves for high reward choices include both High vs. Zero and High vs. Low reward trials.

Multivariate pattern analysis (decoding)

For decoding analyses in both tasks, the main epoch of interest was the 500ms after reward stimulus onset, which provided a window to analyze early representations of reward-associated stimuli ("options" in the reward learning task, "reward cues" in the attention task) in task-relevant and irrelevant contexts. In the attention task, this epoch in the 500/1000ms SOA conditions enabled us to examine the response to the reward stimuli separately from the response to target processing. For completeness, we also examined reward stimulus processing in the 0-500ms after target onset in the 500/1000ms and 0ms SOA conditions.

Decoding was performed on broadband MEG gradiometer data. The true spatial dimensionality of the MEG data after the Maxfilter preprocessing algorithm is ~64 rather than the 204 gradiometer channels (Woolrich et al., 2011). Therefore, to reduce the number of redundant features for decoding, we first performed Principal Component Analysis (PCA) on the data to extract a subset of dimensions (70) that explain 100% of the variance. Note that this simply re-expresses the data using a smaller set of features and does not reduce the number of informative dimensions. Using the 70-feature × N-trial × T-time data matrix as input, we conducted multivariate pattern analysis using Mahalanobis distance with 5-fold cross-validation, an approach closely related to linear discriminant analysis (LDA) (Walther et al., 2016; Wolff et al., 2015, 2017). Specifically, to discriminate between two classes (e.g.,

A and B), we split all of the data into five random groups ("folds") of trials, iteratively using one as a testing set and the remaining as training data (and repeating the splitting procedure 50 times to ensure stable results). We computed Mahalanobis distances between left-out test trials at a given timepoint and the means of class *A* and *B* from the training data at the same timepoint. Mahalanobis distance is given by:

$$Distance_A = \sqrt{(Class\ A_{mean} - test\ trial)^T Cov^{-1} (Class\ A_{mean} - test\ trial)}$$

where Cov^{-1} is the inverse feature covariance estimated on all training data (per time-point, across trials), pooled across classes, using a shrinkage estimator (Ledoit and Wolf, 2004). We then computed the difference between the distances to *A* and *B*, always subtracting the within-class distance from the between-class distance:

$$Distance\ difference = \begin{cases} Distance_B - Distance_A, & if\ test\ trial = Class\ A \\ Distance_A - Distance_B, & if\ test\ trial = Class\ B \end{cases}$$

which leads to positive differences with better discriminability (Wolff et al., 2017). This was repeated for all trials and timepoints and results were smoothed across time with a Gaussian smoothing kernel (σ = 16ms), to obtain a measure of trial-wise pattern discriminability across time. Note that although this distance measure can be binarized and converted to accuracy over trials (as in LDA), we preserved the parametric distance value as a more informative measure of similarity/dissimilarity between train and test patterns (Walther et al., 2016).

We quantified neural pattern separation for various task parameters during the reward learning and attention tasks: reward stimulus location (left versus right; *location decoding*), reward stimulus identity (e.g., high reward stimulus 1 versus high reward stimulus 2; *identity decoding*), and stimulus-independent value (high reward versus low reward; *value decoding*). Location decoding was performed on data collapsed across stimulus identity, and compared between high and low reward trials. Identity decoding was performed separately for each location, with the results averaged over location, and compared between high and low reward trials. For value decoding, we employed a cross-generalisation approach, in which we trained a classifier using one pair of reward stimuli (e.g., high reward 1 vs. low reward 1), and tested performance on another (e.g., high reward 2 vs. low reward 2), collapsing across locations. Value decoding was therefore independent of location and identity, and attributable only to the difference in value between stimuli.

For location and identity decoding in the reward learning task (Fig. 3a-c), the high reward condition included both High vs. Low reward and High vs. Zero reward trials. Value decoding analysis (Fig. 3b) excluded the High vs. Low reward trials to ensure interpretability of results; to obtain equal trial numbers between High vs. Zero and Low vs. Zero trials, we subsampled the latter using an odd/even split. Attention task decoding was performed separately on the 500/1000ms and the 0ms SOA trials.

For statistical testing, we averaged pattern discriminability across trials for each participant and tested it at the group level against zero or between conditions using cluster-corrected sign-permutation tests, with a cluster-forming threshold of α = 0.05 and 10,000 permutations. Baseline data (i.e., before stimulus onset) were not included in permutation testing.

To test how location decoding evolved across trials during the reward learning task as a function of reward (Fig. 3b), for each participant, we computed the Spearman rank

correlation between trial number and peak location decoding in each trial, separately for high and low reward. We tested the average Fisher z-transformed correlation across participants against zero and between reward conditions using one-sample and paired t-tests, respectively. The time of peak decoding was defined based on the group-level decoding results. Note that due to rejection of trials with artefacts, the number of trials included in this analysis is less than in the learning curves presented in Figure 2.

Median split analyses

To test the relationship between the observed decoding and the attentional capture effect in behaviour, we split participant decoding results based on the magnitude of their RT reward × congruency interaction effect across all three SOAs. Decoding differences between groups were tested using independent-samples t-statistics and cluster-corrected group-permutation tests, in which observed group differences were compared to a null distribution of differences generated from random group partitions (cluster-forming $\alpha = 0.05$; 10,000 permutations).

Source reconstruction

Co-registration of MEG sensors and structural MRI was done using OSL (ohba-analysis.github.io). Structural MRI data were bias-corrected and linearly registered to the Montreal Neurological Institute (MNI) space, enabling source reconstruction and analysis to be completed in this common reference space. The MRI scalp surface was extracted and smoothed and fiducial points were manually marked. MRI fiducials were registered to the MEG fiducials using linear transformation and subsequently refined using the iterative closest point algorithm applied to the entire MRI scalp surface and set of Polhemus head shape points. Source reconstruction on MEG gradiometer data was performed in Fieldtrip using a single-shell volume conduction model (based on a mesh of the brain-skull boundary; Nolte, 2003), a leadfield matrix generated from a 10mm-spaced template grid, and linearly constrained minimum variance (LCMV) beamforming (Van Veen et al., 1997). To obtain whole-brain virtual channel data, beamforming filters were applied to time-domain data and, for each gridpoint, the three-direction dipole data were projected to the direction explaining the most variance using singular value decomposition.

Source-space searchlight decoding

To visualize brain regions involved in decoding, we performed searchlight decoding on whole-brain virtual channel data in source space, from 200ms to 500ms after cue onset in 100ms steps. A ~23mm-radius searchlight sphere was used to define features (grid points) for decoding. The sphere was enlarged at the edges of the brain to maintain an approximately constant number of grid points per sphere (across all spheres, M = 62 grid points, SD = 6 grid points). To reduce extensive computation time, the same feature covariance estimate was used for decoding at each time point, which was computed on baseline data (averaged from -100ms to -50ms relative to cue onset). All other aspects of decoding were identical to that described above. For statistical testing, the resultant distance differences were converted into t-statistics and cluster-corrected at the whole-brain level using threshold-free cluster enhancement (TFCE) with 10,000 permutations, as implemented in FSL's *randomise* tool (Smith and Nichols, 2009; Winkler et al., 2014). For visualization, thresholded t-value maps were first interpolated to a 2mm MNI volume using linear interpolation and then interpolated to the Conte69 inflated surface using trilinear interpolation in Fieldtrip (Marcus et al., 2011; Oostenveld et al., 2011).

Code accessibility

Analysis scripts and data will be made available prior to publication.

Results

Reward learning task: Learning stimulus-reward contingencies

We first confirmed that participants learned the stimulus-reward contingencies in the reward learning task. Participants won an average of £44.67 (SD = £2.89) out of a possible £48. Choice accuracy was sensitive to the value difference between options, with a significant main effect of choice type (*high vs. zero*, H-Z; *high vs. low*, H-L; *low vs. zero*, L-Z) on accuracy, $F_{(2,58)} = 7.43$, $p = 0.006$. Participants were more accurate on H-Z than L-Z trials, $t_{(29)} = 4.36$, $p < 0.001$, Cohen's d = 0.8 (Fig. 2a). There was no difference between H-Z and H-L, $t_{(29)} = 1.37$, $p = 0.18$, or H-L and L-Z trials, $t_{(29)} = 2.06$, $p = 0.1$. RT was similarly sensitive to value difference, with a significant main effect of choice type on RT, $F_{(2,58)} = 41.4$, $p < 0.001$. Participants were faster on H-Z and H-L choices than L-Z choices, $t_{(29)} = 7.69$, $p < 0.001$, Cohen's d = 1.4 and $t_{(29)} = 6.07$, $p < 0.001$, Cohen's d = 1.1, respectively (Fig. 2b). There was no difference between H-Z and H-L choices, $t_{(29)} = 1.14$, $p = 0.26$.

Previous work has dissociated the effects of irrelevant reward history and reward-independent selection history on attentional capture (MacLean and Giesbrecht, 2015b). To control for selection history, we doubled the number of Low vs. Zero reward trials to match the choice frequency of low reward options with that of high reward options. We confirmed that choice frequency did not differ between high and low reward options. There was a main effect of stimulus value on choice frequency, $F_{(2,58)} = 721.05$, $p < 0.001$. Participants chose the high and low reward options more frequently than the zero reward stimuli (High vs. Zero, $t_{(29)} = 35$, $p < 0.001$, Cohen's d = 6.39; Low vs. Zero, $t_{(29)} = 28.26$, $p < 0.001$, Cohen's d = 5.15). There was no difference between high and low reward options, $t_{(29)} = 0.6$, $p = 0.55$ (Fig. 2c), demonstrating the absence of a choice frequency (i.e., selection history) effect.

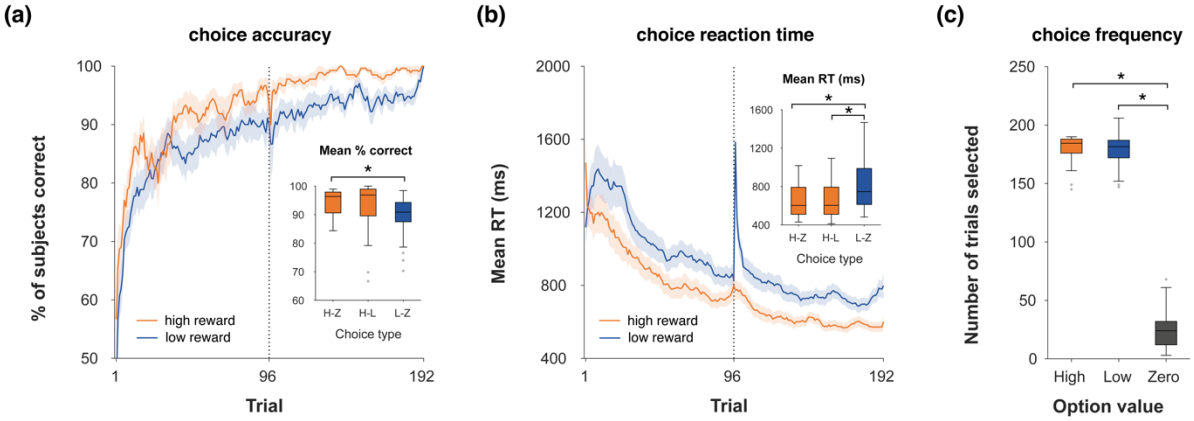

Figure 2. Behavioural results in the reward learning task (training phase). (a) Grand-average learning curves for high-reward (*High vs. Zero, High vs. Low*) and low-reward (*Low vs. Zero*) choice trials. Dotted line indicates the boundary between sessions one and two. Error shading reflects standard error of the mean (SEM). *Inset:* Average percent correct as a function of choice type. H-Z = High vs. Zero; H-L = High vs. Low; L-Z = Low vs. Zero. The central mark within each box indicates the median, the box edges indicate the 25th and 75th percentiles, the whiskers indicate the most extreme data points not considered outliers, and the grey points indicate outliers. Asterisks indicate $p < 0.05$ in a paired t-test. **(b)** Grand-average trial-wise reaction time. Same

conventions as (a). *Inset*: Average reaction time as a function of choice type. Same convention as (a). **(c)** Selection frequency as a function of stimulus value. Same conventions as (a).

Reward learning task: reward stimulus processing in a task-relevant context

Next, we tested the feasibility of time-resolved decoding of reward stimulus representations in the reward learning task, a context in which these stimuli (i.e., *options* for decision-making) are relevant and rewarded. These analyses focused on the fixation epoch, in which participants saw the options but were not yet able to respond.

We applied multivariate pattern analysis to discriminate between trials in which the higher valued option appeared on the left versus the right of the fixation cross, separately for the high and low reward trials (*location decoding;* Fig. 3a). Given the obvious perceptual differences between left and right option trials, we expected the decoding analysis to reflect this. Crucially, however, these perceptual differences should be identical in high and low reward trials, and therefore any differences in decoding between these conditions are attributable solely to the reward associated with each type of option. As expected, for both high- and low-reward options, we could decode option location from ~104ms and ~136ms onwards, respectively (each $p < 0.001$, cluster-corrected permutation test), in line with the clear perceptual difference between left and right cue presentation trials. Critically, the decoding was significantly stronger for the high- than the low-reward options from ~184ms onwards ($p < 0.001$, cluster-corrected permutation test), indicating that learned value modulated location decodability in this task-relevant context (Fig. 3a). This is consistent with an effect of reward on spatial attention (Anderson, 2016; MacLean et al., 2016; Moore and Zirnsak, 2017).

Given that participants gradually learned to locate and select the higher reward stimulus, we examined how location decoding emerged across trials as a function of associated reward. We extracted trial-wise distance differences from the peak time point of maximal decoding in the trial-averaged data in the high and low reward conditions (i.e., Fig. 3a) and tested for a relationship with trial number. In line with participants' learning, location decoding significantly increased over trials in the high reward condition (t-test on the participant-wise, Fisher z-transformed Spearman rank correlations; $t_{(29)} = 8.58$, $p < 0.001$; see also Fig. 3b top) and in the low reward condition ($t_{(29)} = 2.09$, $p = 0.0458$; see also Fig. 3b bottom). Correlations were stronger in the high reward compared to the low reward condition ($t_{(29)} = 5.54$, $p < 0.001$; Fig. 3b inset). Thus, the emergence of location decoding across trials also differed as a function of associated reward, consistent with the idea that reward learning gradually shapes selective attention (Anderson, 2016; Chelazzi et al., 2013).

Next, we applied a similar multivariate pattern analysis to discriminate between the two stimulus identities within each reward condition (e.g., high reward 1 vs. high reward 2; *identity decoding*; Fig. 3c). Identity could be decoded from ~80ms and ~104ms onwards for high and low reward stimuli, respectively ($p < 0.001$, cluster-corrected permutation test), but with no difference between reward conditions ($p > 0.9$, cluster-corrected permutation test), suggesting that learned value did not modulate the sensory representations of these stimuli in this task (Fig. 3c).

Lastly, we sought to decode a reward value signal, independent of location or identity. We used a cross-generalisation approach, in which we trained a classifier using one pair of reward stimuli (e.g., high 1 vs. low 1), and tested performance on another (e.g., high 2 vs.

low 2), collapsing across locations (e.g., Kahnt et al., 2010). Any significant decoding that emerges is therefore independent of location and identity, and so attributable to the difference in value between stimuli (*value decoding;* Fig. 3d). We found a significant value signal from ~260ms onwards ($p < 0.001$, cluster-corrected permutation test), representing the available reward independently of stimulus location or identity (Fig. 3d).

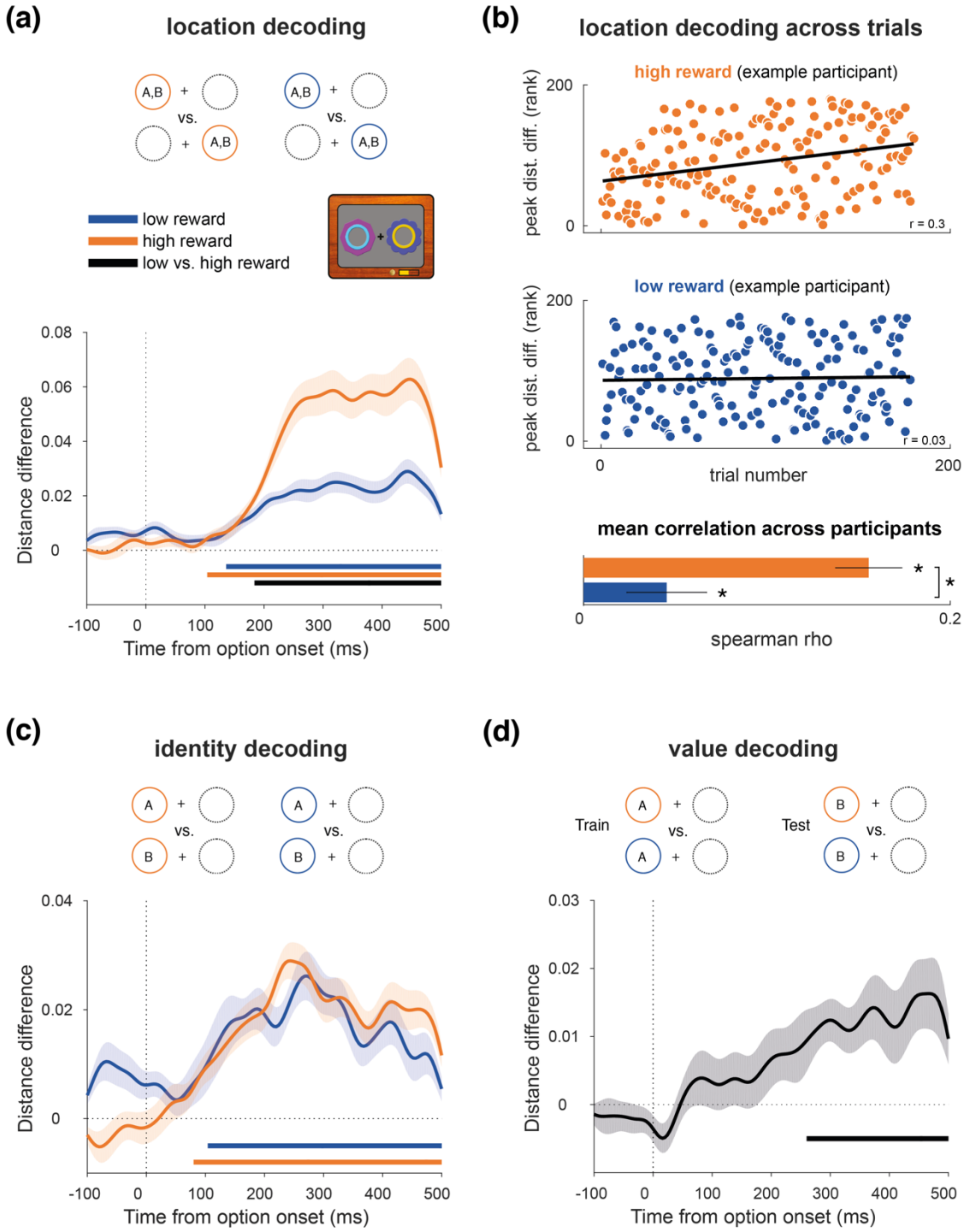

Figure 3. Decoding reward option location, identity, and value in the reward learning task. (a) Decoding the location of the reward-associated stimuli involved discriminating between trials in which the higher reward stimulus appeared on the left versus right, collapsing across stimulus identities. Curves depict decoding

averaged across trials and participants for high and low reward options. Bars indicate significant decoding ($p < 0.05$, cluster-based permutation test across time) for each reward condition (orange, blue bars) and between reward conditions (black bar). Shaded regions indicate SEM. **(b)** Correlation between location decoding at peak and trial number in the high and low reward conditions. Scatter plots show ranked peak decoding across trials for one example participant, together with the corresponding trend lines. Bar plot shows mean Fisher z-transformed Spearman correlation for each condition, across all participants. **(c)** Decoding the identity of reward-associated stimuli involved discriminating between trials with distinct stimulus identities for each reward value, within each location with results averaged across (only one location depicted in schematic). Same conventions as Figure 3a. **(d)** Decoding reward value involved using one pair of high and low reward stimuli as training data and a different pair as testing data (collapsing across location); any signal that generalises across pairs is independent of stimulus identity or location and can therefore be attributed to the difference in value between high and low reward stimuli. Same conventions as Figure 3a.

Attention task: Attentional capture by stimuli associated with reward history

Next, we probed how stimulus-reward associations learned in the reward learning task captured attention in the attention task and whether attentional capture was modulated by reward value and/or by the SOA. We ran a repeated-measures ANOVA on RT with three factors: *reward* (high, low), *congruency* (congruent, incongruent), and *SOA* (0, 500, 1000ms). There was a main effect of congruency, $F_{(1,29)} = 12.46$, $p = 0.001$ and a congruency × reward interaction, $F_{(1,29)} = 8.9$, $p = .006$. Participants were significantly slower in the high reward incongruent relative to the congruent condition, $t_{(29)} = 3.77$, $p = 0.002$, Cohen's $d = 0.69$, with no such difference between the low reward incongruent and congruent conditions, $t_{(29)} = 1.77$, $p = 0.087$, Cohen's $d = 0.32$. Importantly, although there was a main effect of SOA, $F_{(2,58)} = 44.33$, $p < 0.001$ (indicative of a general preparatory effect), there were no interactions between SOA and reward or congruency, all $F_{(2,58)} < 1$, $p > 0.3$. For completeness, we tested for reward × congruency effects in each SOA. Across SOA conditions, participants were slower in the high-reward incongruent trials than the congruent trials: *0ms SOA*, $t_{(29)} = 4.55$, $p = 0.001$, Cohen's $d = 0.83$; *500ms SOA*, $t_{(29)} = 3.15$, $p = 0.019$, Cohen's $d = 0.57$; *1000ms SOA,* $t_{(29)} = 2.8$, $p = 0.036$, Cohen's $d = 0.51$ (Figure 4a). There was no difference between low-reward incongruent and congruent trials, all $t_{(29)} < 2$, $p > 0.2$ (Figure 4a).

A congruency effect on reaction time could be driven both by faster responses in congruent trials, and/or slower responses in incongruent trials, compared to baseline. Figure 4a suggests that both might be the case, and we next tested this explicitly. Given the absence of interactions with SOA, we collapsed across this condition and performed one-sample t-tests for each congruency and reward condition. In high-reward trials, participants showed both a congruent ($t_{(29)} = 3.14$, $p = 0.004$, Cohen's $d = 0.57$) and incongruent effect ($t_{(29)} = 2.59$, $p = 0.015$, Cohen's $d = 0.47$), suggesting that they were respectively sped up or slowed down by the presence of a congruent or incongruent high-reward stimulus. These effects were not present in the low-reward conditions ($t_{(29)} = 1.2$, $p = 0.238$; and $t_{(29)} = 1.38$, $p = 0.178$, respectively).

We then tested whether the effect of congruency on RT decayed over trials, as participants repeatedly encountered the unrewarded and irrelevant stimuli. This would reflect an extinction of the stimulus-reward association as reward becomes unavailable, as widely observed in learning paradigms (Todd et al., 2014). Focusing on the high reward condition and collapsing across SOAs, we split trial data into two halves per session and computed a difference between congruent and incongruent RTs as an aggregate measure of attentional capture for each half. A *session* × *half* repeated-measures ANOVA showed no significant main effects or interactions, all $F_{(1,29)} < 2.8$, $p > 0.11$, suggesting that the effect did not reliably extinguish across trials within the timeframe of this experiment (see also Figure 4b).

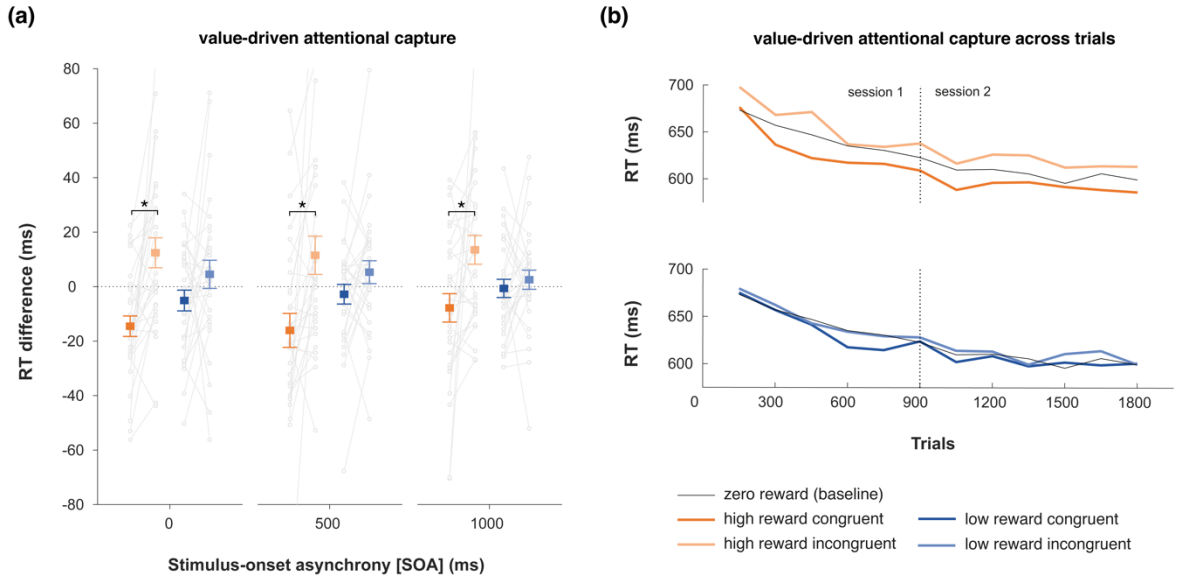

Figure 4. Value-driven attentional capture as measured by behaviour in the attention task. (a) Mean RT difference scores (with baseline condition subtracted out) as a function of reward, congruency, and SOA. Grey lines indicate individual participant data. Positive and negative values indicate RTs slower and faster than baseline, respectively. Asterisks indicate $p < 0.05$ in a paired t-test. Error bars indicate SEM. **(b)** RTs for each condition across trials, averaged within 150-trial bins.

We also analysed accuracy difference scores. There was a significant main effect of congruency, $F_{(1,29)} = 9.25$, $p = 0.005$; a main effect of SOA, $F_{(2,58)} = 3.17$, $p = 0.049$; a reward × congruency interaction, $F_{(1,29)} = 20.11$, $p = 0.0001$; and a reward × congruency × SOA interaction, $F_{(2,58)} = 3.21$, $p = 0.047$. In the high reward 500ms and 1000ms SOA conditions only, participants were less accurate in the incongruent than in the congruent trials, $t_{(29)} = 3.75$, $p = 0.005$, Cohen's $d = 0.68$ and $t_{(29)} = 3.45$, $p = 0.009$, Cohen's $d = 0.63$. There were no differences in the 0ms SOA or in any low reward condition, all $t_{(29)} < 2$, $p > 0.9$. Thus, attentional capture also influences accuracy, at least in the longer SOA conditions, with no evidence of a speed-accuracy trade-off.

Reward cue location is decodable in a task-irrelevant context and modulated by value

Next, we probed the neural correlates of the attentional capture effect we observed in behaviour. We aimed to identify neural signatures of task-irrelevant reward history, independently of target processing. Similar to the analysis of the reward learning task data, we performed time-resolved decoding of the location and identity of the reward cues, as well as a stimulus-independent value signal. This enabled us to probe the time-course of any effects of reward history, such as modulations in early visual processing. Our primary focus was the cue epoch, prior to the onset of task-relevant gratings, as this period allowed for the analysis of task-irrelevant reward cue processing without the interference of target processing. We specifically focused on the first 500ms after reward cue onset as this allowed us to collapse across the 500ms and 1000ms SOA trials.

We first looked at location decoding as the most direct correlate of the spatially-specific attentional capture effects that we observed in behaviour. As before, we found significant

decoding of the cue location for both high ($p < 0.001$, cluster-corrected permutation test) and low reward cues ($p < 0.001$, cluster-corrected permutation test; Fig. 5a). Critically, this decoding was modulated by reward value, with stronger decoding for high compared to low reward cues starting from ~260ms ($p < 0.001$, cluster-corrected permutation test; Fig. 5a). This effect is solely attributable to the reward history that these stimuli acquired during the reward learning task; in the current context, these stimuli are unrewarded and irrelevant.

We sought to determine the anatomical source of this value modulation. We projected the sensor-space data onto a source-space grid using a linearly constrained minimum variance (LCMV) beamformer, and ran the same location decoding analysis within a searchlight sphere across the brain, in 50ms bins from 250-500ms after cue onset. Value modulation began around the right posterior parietal cortex, followed by the inferior temporal and visual cortex and more widespread modulation in posterior parietal cortex, and along the temporal lobe ($p < 0.05$, whole-brain cluster-corrected using TFCE; Fig. 5b).

We then tested whether this value modulation was related to the value modulation of the behavioural attentional capture effect. We conducted a median split of the participants based on the extent to which their attentional capture was modulated by reward value (i.e., the strength of the reward × congruency interaction effect on RT; Fig. 5d top panel). Strong capture participants (i.e., with stronger value modulation of the attentional capture effect) showed accompanying value modulation of the location decoding during the cue epoch starting from ~248ms ($p < 0.001$, cluster-corrected permutation test; Fig. 5c bottom panel), while weak capture participants did not ($p = 0.215$, cluster-corrected permutation test; Fig. 5c top panel), with a significant difference between these two groups ($p = 0.024$, cluster-corrected, independent-samples permutation test; Fig. 5d bottom panel). We defined these two groups based on the extent to which reward value modulates the behavioural effects of attentional capture, but they might also differ in how they learn reward associations (e.g., Jahfari and Theeuwes, 2017). We therefore compared their learning curves from the reward learning task, but did not find any significant differences ($p = 0.423$, independent-samples cluster-corrected permutation test across trials; Fig. 5d middle panel).

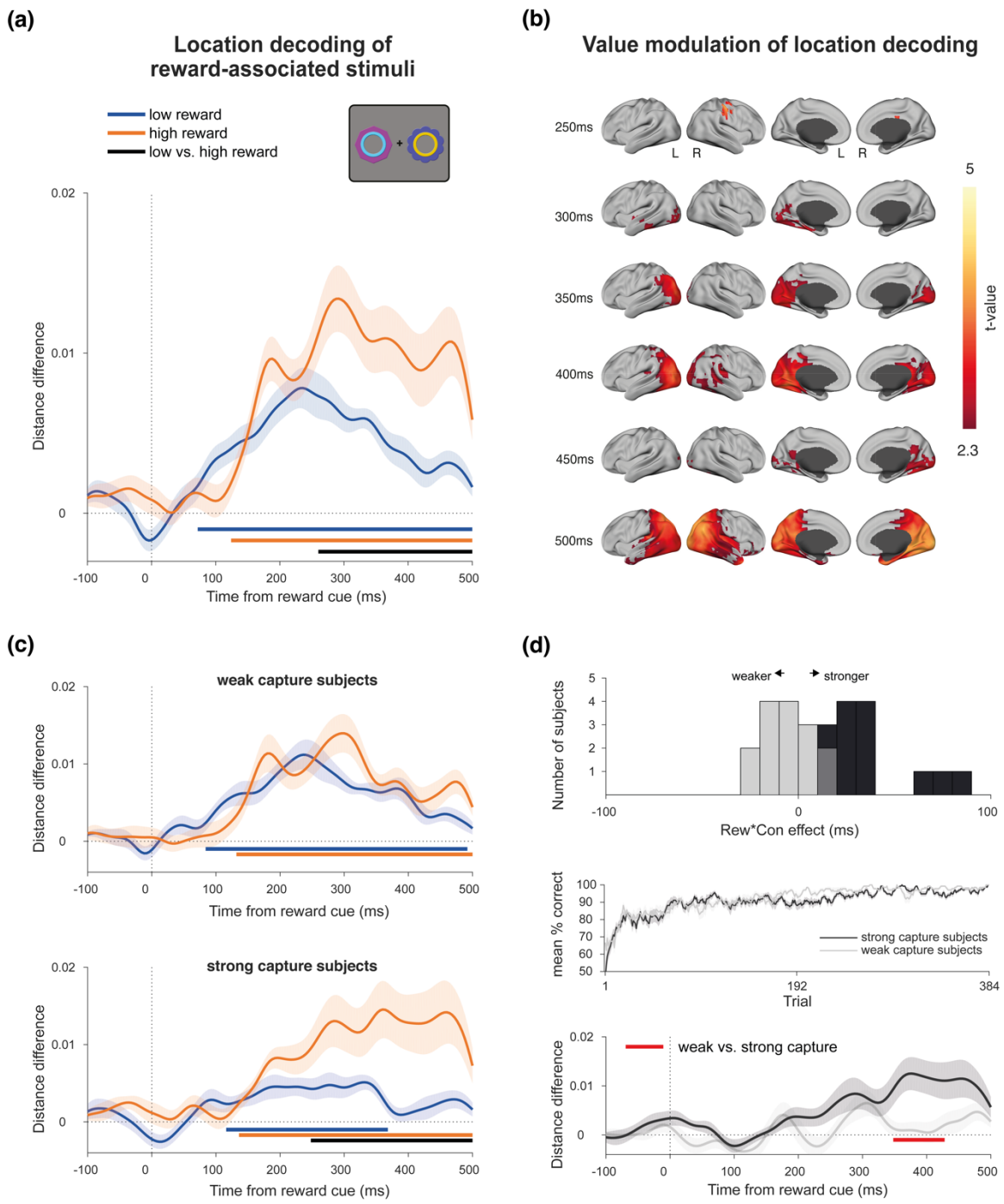

Figure 5. Decoding reward cue location in the attention task during the cue epoch of the 500ms and 1000ms SOA conditions. (a) Decoding of reward cue location during the cue epoch for high- and low-reward stimulus trials. Same conventions as Figure 3a. **(b)** Significant value modulation of location decoding in a source-space searchlight analysis. Maps depict t-statistics at selected time-points during the cue epoch, and are thresholded at $p < 0.05$, whole-brain cluster-corrected using TFCE. **(c)** Same decoding as (a) but performing a median split on the participant-level data according to each participant's reward × congruency behavioural effect (i.e., value-modulated attentional capture effect; see Figure 5d). *Top*: the "weak capture" group. *Bottom*: the "strong capture" group. **(d)** Behavioral and decoding comparison of each participant group from (c). *Top*: histogram of participants' reward × congruency behavioural effect (weak capture in grey, strong capture in black). *Middle*: learning curves for each group. Same color conventions as above. *Bottom*: Differences between high- and low-reward location decoding (orange minus blue lines) for each group from (c). Same color

conventions as above. Red bar indicates significant difference between groups ($p < 0.05$, independent-samples cluster-based permutation test across time).

Next, we tested whether the cue location decoding persisted into the target epoch, which would suggest that participants maintain traces of the irrelevant reward cue location even while discriminating the oriented gratings. We repeated the location decoding on 500ms and 1000ms SOA trial data, now time-locked to the grating onset. We again found significant decoding of cue location for both high ($p < 0.001$, cluster-corrected permutation test) and low reward cues ($p < 0.001$, cluster-corrected permutation test), which was also modulated by reward value ($p < 0.001$, cluster-corrected permutation test; Fig. 6a). Note that the significant decoding prior to grating onset (the typical "baseline" period) occurs because this period overlaps with the preceding cue epoch. As above, we tested whether this value modulation during the target epoch related to the behavioural attentional capture effect. A median split analysis (described above) showed that strong capture participants had significant value modulation of location decoding during the target epoch ($p = 0.001$, cluster-corrected permutation test), while weak capture participants showed a similar trend ($p = 0.063$, cluster-corrected permutation test; Fig. 6b). The difference between these two groups, however, was not significant ($p = 0.223$, cluster-corrected, independent-samples permutation test).

We also performed the same location decoding analysis in the 0ms SOA condition, in which reward cues and gratings are presented simultaneously. We found significant decoding of the cue location for high ($p < 0.001$, cluster-corrected permutation test) but not low reward cues ($p = 0.12$, cluster-corrected permutation test), and a significant value modulation from ~224ms ($p = 0.02$, cluster-corrected permutation test; Fig. 6c). As before, we conducted a median split analysis (described above). However, we did not find value modulation of the location decoding when analysing each group separately ($p = 0.335$ and $p = 0.12$, respectively, cluster-corrected permutation tests; Fig. 6d). Note that these analyses should be interpreted with caution because of simultaneous cue and target processing in this condition as well as the reduced within-subject power, with half as many trials here as in the combined 500ms and 1000ms SOA decoding.

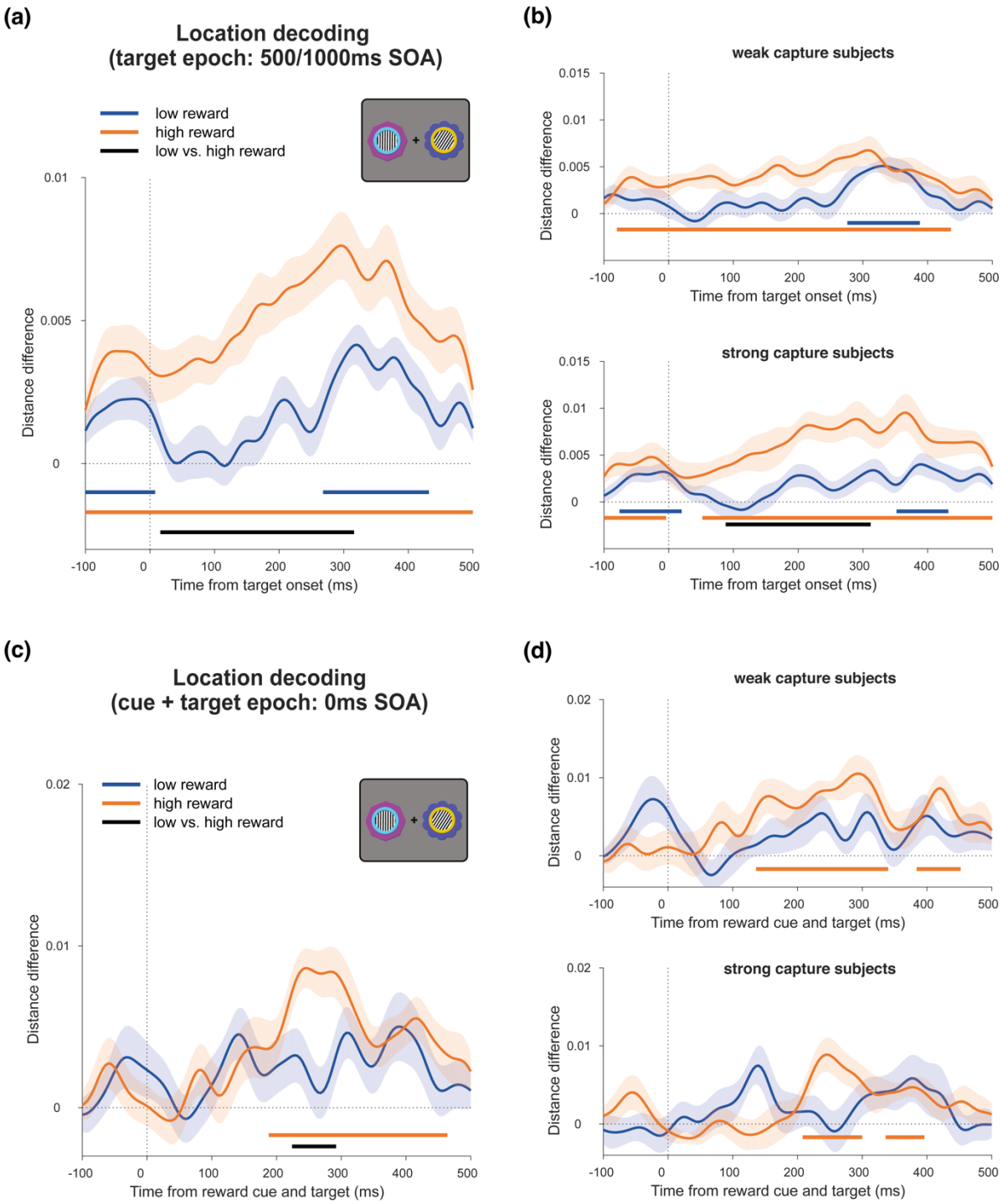

Figure 6. Decoding reward cue location in the attention task during the target epoch. (a) Decoding of reward cue location in the target epoch in the 500ms and 1000ms SOA trials. Note that significant decoding in the baseline period is due to the temporal overlap with the cue epoch. Same conventions as Figure 3a. **(b)** Same decoding as (a) but performing a median split on the participant-level data according to each participant's reward × congruency behavioural effect (see Figure 5c-d for details). **(c-d)** Same analysis as (a-b) but for the 0ms SOA condition (simultaneous cue and target onset).

Reward cue identity decoding is not modulated by value in a task-irrelevant context

In addition to the location decoding of the reward cues (i.e., reflecting spatial selection), it is possible that decoding of the cue identities (putatively reflecting visual feature

representations) would be modulated by learned value (Anderson, 2016; Failing and Theeuwes, 2018). Although we did not observe an effect of reward value on identity decoding during the reward learning task, we nevertheless explored this possibility during the attention task. Although we could reliably decode identity for each type of reward cue (high reward, from ~128ms, $p < 0.001$, cluster-corrected permutation test; low reward, from ~124ms, $p < 0.001$, cluster-corrected permutation test), this was not modulated by value ($p = 0.153$, cluster-corrected permutation test; Figure 7a). When we performed a median split analysis by behaviour (described above), the strong capture participants showed a hint of value modulation from ~168ms, with worse decoding for the high reward cues, but this was not significant ($p = .066$, cluster-corrected permutation test; Figure 7b bottom panel). Weak capture participants did not show any value modulation ($p = 0.325$, cluster-corrected permutation test; Figure 7b top panel). A similar pattern was observed when decoding in the 0ms SOA trials, with significant decoding of stimulus identity in high and low reward trials (for both, $p < 0.001$, cluster-corrected permutation test), but no significant value modulation ($p > 0.9$, cluster-corrected permutation test; Figure 7c). Likewise, neither strong nor weak capture participants showed significant value modulation (strong capture: $p = 0.572$; weak capture: $p > 0.9$, cluster-corrected permutation tests; Figure 7d).

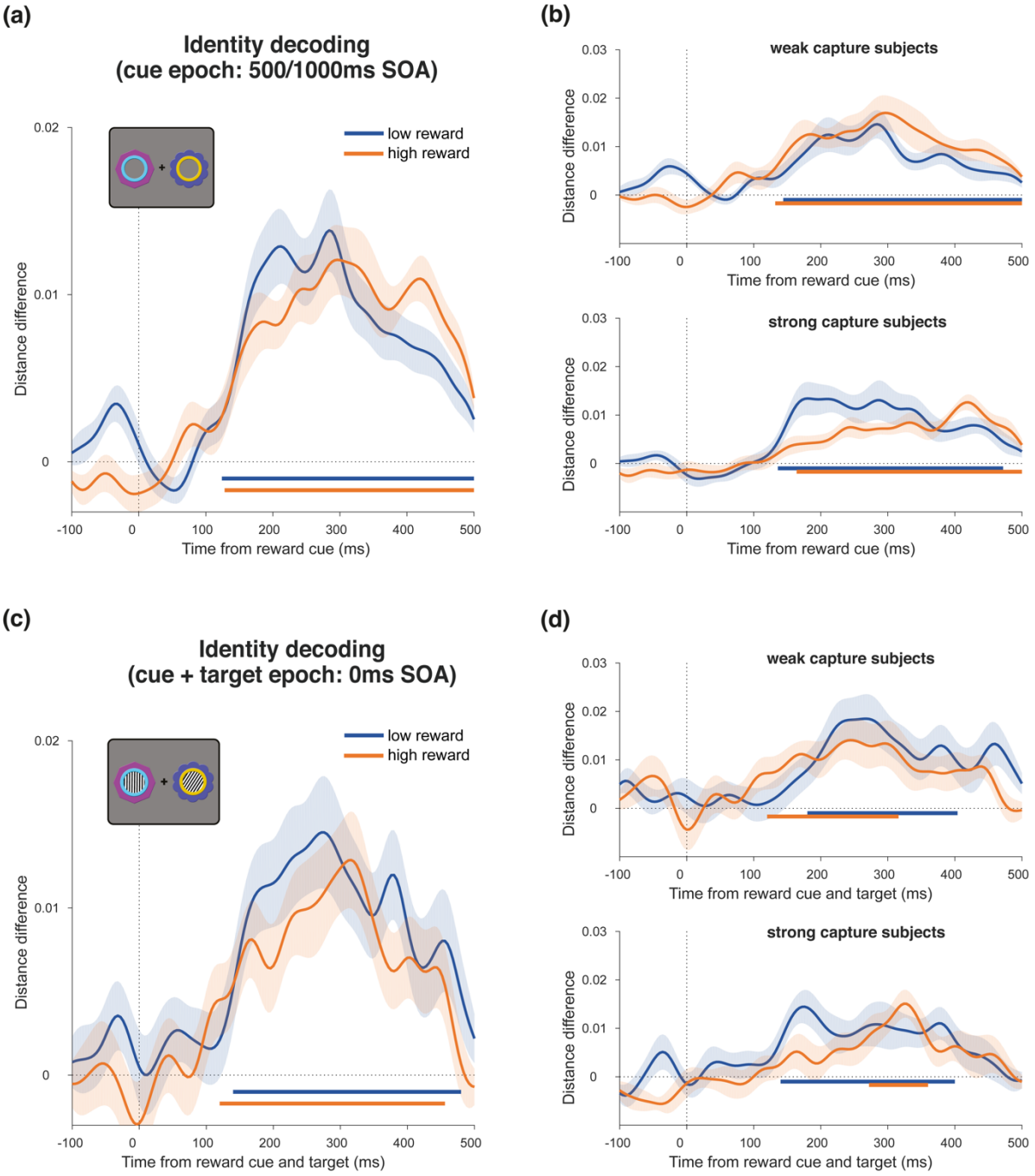

Figure 7. Decoding reward cue identity in the attention task. (a) Decoding of reward cue identity during the cue epoch in the collapsed 500ms and 1000ms SOA conditions. Same conventions as Figure 3a. **(b)** Same decoding as (a) but performing a median split on the participant-level data according to each participant's reward × congruency behavioural effect (see Figure 5c-d for details). **(c-d)** Same analysis as (a-b) but for the 0ms SOA condition.

It is possible that any effect of reward history on identity decoding is confined to a specific anatomical region (e.g., within the ventral visual stream), which our whole-brain sensor-space analysis may have missed. To test this, we repeated the analysis using source-space searchlight decoding across the brain in 50ms time steps from cue onset and tested for significant clusters. There were no significant differences between high and low reward trials anywhere in the brain (500ms and 1000ms SOA: $p > 0.1$; 0ms SOA: $p > 0.209$; whole-brain

cluster-corrected using TFCE). Thus, we did not find any evidence that reward history modulates stimulus identity representations in either a task-relevant, or a task-irrelevant context in the current experiment. Moreover, any hint of an effect is in the opposite direction to that expected, with slightly worse decoding in the high reward condition.

Decoding stimulus-independent reward value in a task-irrelevant context

Finally, we sought to decode a location- and identity-independent value signal during the attention task, which would provide additional evidence that value information continues to be represented in a task-irrelevant context. Using the same cross-generalisation approach as before, we found significant value decoding in the cue epoch, emerging from ~336ms ($p = .005$, cluster-corrected permutation test; Fig. 8a). In a median split analysis based on participants' behaviour (described above), neither the strong nor the weak capture group showed significant decoding by itself (strong capture: $p = .088$; weak capture: $p = 0.146$, cluster-corrected permutation tests), although the strong capture participants appeared to be driving the overall effect (Fig. 8b). The difference between groups was not significant ($p > 0.9$, independent-samples cluster-corrected permutation test). The absence of significant decoding in either of the two subgroups, together with significant decoding across the entire sample, is most likely explained by a lack of statistical power in the former analysis, rather than a true null effect. Source-space searchlight decoding of this value signal across the brain showed significant clusters in bilateral visual, left inferior temporal, and left inferior frontal cortex ($p < 0.05$, whole-brain cluster-corrected using TFCE; Fig. 8c). In the 0ms SOA condition, we found no significant value decoding at any timepoint ($p > 0.9$, cluster-corrected permutation test).

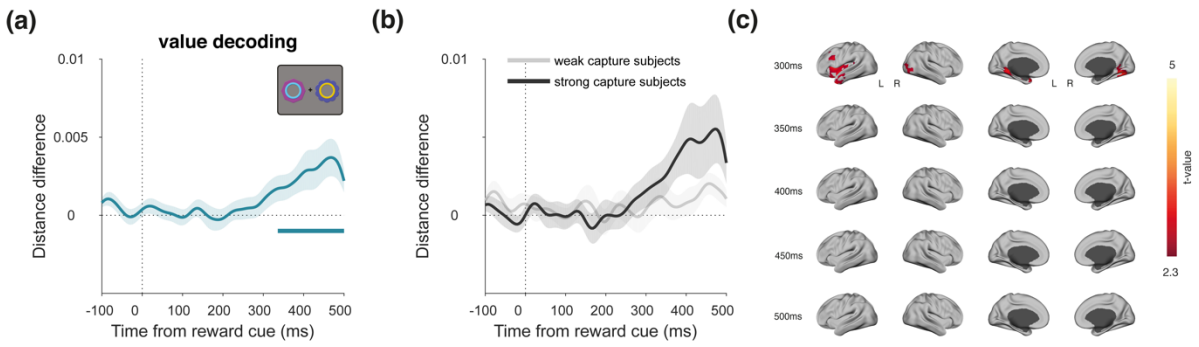

Figure 8. Value decoding in the attention task during the cue epoch of the 500ms and 1000ms SOA conditions. (a) Value decoding during the cue epoch in the collapsed 500ms and 1000ms SOA conditions. Same conventions as Figure 3a. **(b)** Same decoding as (a) but performing a median split on the participant-level data according to each participant's reward × congruency behavioural effect (see Figure 5c-d for details). **(c)** Significant value decoding in a source-space searchlight analysis at selected time-points. Same conventions as Figure 5b.

Discussion

We recorded brain activity using MEG as participants completed a reward learning task to establish stimulus-reward associations, followed by an attention task to measure VDAC. First, we showed a spatially specific behavioural VDAC effect, with reward-associated stimuli respectively speeding or slowing RT in congruent and incongruent trials, consistent with attentional costs and benefits (Failing and Theeuwes, 2014; Posner, 1980). This effect was modulated by reward value, suggesting that it is the associated *value* that is driving

capture, rather than non-specific selection history (MacLean and Giesbrecht, 2015b). Importantly, VDAC was robust even with a delay between reward-associated stimuli and targets (see also Failing and Theeuwes, 2015), allowing us to isolate processing of reward-associated stimuli with MEG.

Using time-resolved MVPA, we found that location decoding of task-irrelevant reward cues was modulated by value from ~260ms after stimulus onset. Searchlight decoding of source-space data localised this value modulation to posterior parietal, temporal, and visual cortex. This neural effect was related to behaviour: participants who had strong VDAC also had larger value modulation of location decoding. Further, we find that the value modulation of location decoding extended into the target epoch, consistent with the behavioural effects of VDAC observed in the long SOA conditions (500ms and 1000ms). We found an additional value signal in the long SOA conditions, which was independent of the location or identity of the reward stimuli. Source-space decoding localised this effect to visual, temporal, and inferior frontal cortex. In contrast, although we could decode the identity of reward cues, this decoding was not modulated by value. This was the case regardless of SOA condition; whether we focused our analysis on participants showing a strong VDAC effect; or whether we performed decoding on whole-brain data or with searchlight analysis.

Value signals and spatial attention

The timing of the value modulation of location decoding is consistent with studies showing a lateralised N2pc signal for reward-associated stimuli (Hickey et al., 2010; Itthipuripat et al., 2015; Qi et al., 2013). These results suggest an effect of value on spatial attention (MacLean et al., 2016; Moore and Zirnsak, 2017; Woodman and Luck, 1999). Moreover, localisation of this effect to the posterior parietal cortex (PPC) is in line with theories proposing that regions in this area (e.g., the lateral intraparietal area [LIP] in monkeys) integrate diverse signals, including task information and physical salience, to determine the overall attentional priority of stimuli (Bisley and Goldberg, 2010; Zelinsky and Bisley, 2015). Single-unit recording and fMRI studies suggest that learned reward value is also a prominent signal integrated in the PPC (Anderson et al., 2014; Barbaro et al., 2017; Ghazizadeh et al., 2018; Gottlieb and Snyder, 2010). For example, LIP neurons encode learned value even when this interferes with goal-oriented behaviour, and such biases transfer to a task-irrelevant context after extensive training (Peck et al., 2009). Interestingly, after the onset of task-irrelevant reward cues, LIP neurons show sustained increases in firing rate for at least 800ms (Peck et al., 2009). This dovetails with our findings that the behavioural effects of VDAC are also present at long SOAs and that value modulation of attention extends into the target epoch.

The spatial resolution of source localization in the current study was insufficient to confidently distinguish sub-regions within the parietal cortex (Corbetta and Shulman, 2002). Indeed, our findings are also consistent with studies showing that ventral parts of the PPC, such as the inferior parietal lobule (IPL), are involved in the detection of salient events and attentional orienting (Corbetta and Shulman, 2002; Husain and Nachev, 2007). The processing of reward history in this area is not well understood (Frank and Sabatinelli, 2012). The relative contributions of parietal sub-regions throughout the time-course of VDAC remains an important open question.

Value modulations in the ventral visual stream are similarly consistent with attentional effects, particularly given their late timing (see also below; Buffalo et al., 2010; Foxe and Simpson, 2002). A stimulus-independent value signal was also present in the inferior frontal

cortex and neighbouring anterior insula. Wang et al. (2015) found that the anterior insula was specifically activated when reward-associated distracters were contrasted according to their value (high versus low reward), irrespective of their spatial location. One theory of anterior insula function suggests that it is involved in signalling salient events in the environment (Corbetta and Shulman, 2002; Downar et al., 2000; Menon and Uddin, 2010). Our findings are in line with this idea, although the late timing of observed value signals precludes strong interpretation of their functional role.

The latency of value signals and VDAC

The latency of value signals observed in our study is too late to suggest a causal role in modulating visual processing. Attentional modulations arising from frontal and parietal cortex—the putative effects of VDAC—have been shown to already occur by ~250ms (Anderson, 2016; Buffalo et al., 2010; Foxe and Simpson, 2002). Indeed, robust behavioural effects are also observed when targets are presented simultaneously to the reward stimuli (e.g., 0ms SOA condition; see also Anderson et al., 2011). In these trials, it is likely that any value signal would have to occur earlier than ~200ms to causally influence visual processing (Buffalo et al., 2010; Foxe and Simpson, 2002). It is possible that there is an early cortical effect which we cannot detect due to a lack of power. As described earlier, some EEG studies do report value modulation from ~100ms (Hickey et al., 2010; Luque et al., 2017; MacLean and Giesbrecht, 2015a).

Differences in task design could potentially explain the discrepancies between studies. For example, the P1 effect in Hickey et al. (2010) was observed using an inter-trial priming paradigm in which the reward history and task relevance of stimuli changed across trials. Notably, MacLean and Giesbrecht (2015a) did find a value modulation of the P1 component days after reward learning. However, it only occurred in trials in which the reward-associated stimulus directed attention towards the target, suggesting that it interacted with task relevance (MacLean and Giesbrecht, 2015a). Similarly, the P1 effect in Luque et al. (2017) occurs in the outcome phase of a reinforcement learning task in which stimuli are task-relevant. A recent study reported value modulations of neurons in macaque area TE as early as ~81ms after visual onset, although this was also in a task-relevant decision-making context (Sasikumar et al., 2018). In contrast, in the current study and in Qi et al. (2013), who did not find a P1 effect, the reward-associated stimuli were entirely irrelevant in the attention task. Therefore, it is possible that early cortical value signals may only be present, or at least detectable, when they coincide with current or recent task-related attentional modulation (Failing and Theeuwes, 2018).

Implications for the visual cortical plasticity account

According to the visual cortical plasticity account of VDAC, value may be directly encoded in cortex via plasticity of stimulus representations in the ventral visual stream (Anderson, 2016; Failing and Theeuwes, 2018; van Koningsbruggen et al., 2016). High-level object, perceptual, and category learning are known to induce plasticity throughout the ventral visual stream and higher-order areas (Frankó et al., 2010; LeMessurier and Feldman, 2018; Miyashita, 1988; Op de Beeck and Baker, 2010; Poort et al., 2015; Schoups et al., 2001; Srihasam et al., 2014). It is possible that such changes can underlie value modulation of early visual processing during VDAC, such as the P1 effects described above. Increased decodability of reward-associated stimuli (e.g., Hickey and Peelen, 2015) has also been taken as supporting evidence (Failing and Theeuwes, 2018). Importantly, Hickey and Peelen (2015)

were decoding object categories. In the current study, we specifically focused on within-category stimulus identity and did not observe value modulation of identity decoding in either the reward learning or attention task. Moreover, in line with previous research on VDAC (e.g., Anderson et al., 2011; Hickey and Peelen, 2015), reward learning in the current study was conducted over a short timescale relative to perceptual learning studies, which typically require multiple training sessions over several days (e.g., Poort et al., 2015; Schoups et al., 2001). Therefore, it remains unclear whether visual cortical plasticity can occur under the same timescale as VDAC.

Subcortical value signals

Alternatively, it is possible that VDAC may be explained by plasticity in subcortical regions (Anderson, 2016; Hikosaka et al., 2018), to which MEG is relatively insensitive (Hillebrand and Barnes, 2002). A key subcortical route may be a recently identified circuit involved in rapid orienting to reward-associated stimuli (Hikosaka et al., 2018). This circuit includes the tail of the caudate nucleus (CDt), whose neurons are object- and spatially-selective, as well as the substantia nigra pars reticulata, and the superior colliculus (Griggs et al., 2018; Yamamoto et al., 2012, 2013; Yasuda and Hikosaka, 2015). Learned value modulates neural activity in each of these regions (Hikosaka et al., 2018). Value information from this circuit can reach the cortex via the thalamus (Ahmadlou et al., 2018; Berman and Wurtz, 2010), which is itself an important hub for attentional control (Saalmann and Kastner, 2009), and has been recently shown to encode long-term value associations (Yasuda and Hikosaka, 2018).

Multiple parallel pathways are possible (Hikosaka et al., 2018). Indeed, despite the CDt's sensitivity to learned value, inhibiting this area surprisingly does not affect saccades to reward-associated stimuli (Kim and Hikosaka, 2013). Certain models of cortico-basal ganglia interactions suggest that value signals may first be encoded in the basal ganglia, which then gradually trains cortical networks to form associative links between stimulus features and values; after extended learning, cortical plasticity may be sufficient to drive VDAC (Hélie et al., 2015; Houk and Wise, 1995). Consistent with this, neurons in LIP and extrastriate cortex show a training-dependent latency shift in value coding, with early signals (e.g., earlier than 200ms) appearing after days of training (Frankó et al., 2010; Peck et al., 2009). Thus, it is possible that with longer training we would have observed earlier cortical value signals in the current study.

The amygdala is another candidate region, with its neural activity encoding spatial and reward information which correlates with spatial attention effects in behaviour (Chau et al., 2015; Leathers and Olson, 2017; Peck and Salzman, 2014; Peck et al., 2014; Vuilleumier, 2015). Lastly, although not technically subcortical, the hippocampus is also an area of interest which shows value coding, particularly after long-term learning (Lebreton et al., 2009; Merre et al., 2018; Wimmer et al., 2018). The role of subcortical and other regions in the interaction between reward learning and attention is only beginning to be explored and deserves future study (Arcizet and Krauzlis, 2018; Griggs et al., 2018; Hikosaka et al., 2018).

Conclusion

Overall, our results suggest that VDAC is underpinned by learned value signals which modulate spatial selection throughout posterior visual and parietal cortex. However, despite

previous studies suggesting an important role for early cortical plasticity, we suggest that VDAC can occur in the absence of changes in early visual cortical processing.

References

Ahmadlou, M., Zweifel, L.S., and Heimel, J.A. (2018). Functional modulation of primary visual cortex by the superior colliculus in the mouse. Nature Communications *9*, 3895.

Anderson, B.A. (2013). A value-driven mechanism of attentional selection. J Vis *13*.

Anderson, B.A. (2016). The attention habit: how reward learning shapes attentional selection. Ann. N. Y. Acad. Sci. *1369*, 24–39.

Anderson, B.A., Laurent, P.A., and Yantis, S. (2011). Value-driven attentional capture. Proc. Natl. Acad. Sci. U.S.A. *108*, 10367–10371.

Anderson, B.A., Laurent, P.A., and Yantis, S. (2014). Value-driven attentional priority signals in human basal ganglia and visual cortex. Brain Res. *1587*, 88–96.

Arcizet, F., and Krauzlis, R.J. (2018). Covert spatial selection in primate basal ganglia. PLOS Biology *16*, e2005930.

Awh, E., Belopolsky, A.V., and Theeuwes, J. (2012). Top-down versus bottom-up attentional control: a failed theoretical dichotomy. Trends Cogn. Sci. (Regul. Ed.) *16*, 437–443.

Barbaro, L., Peelen, M.V., and Hickey, C. (2017). Valence, Not Utility, Underlies Reward-Driven Prioritization in Human Vision. J. Neurosci. *37*, 10438–10450.

Beck, D.M., and Kastner, S. (2009). Top-down and bottom-up mechanisms in biasing competition in the human brain. Vision Research *49*, 1154–1165.

Berman, R.A., and Wurtz, R.H. (2010). Functional Identification of a Pulvinar Path from Superior Colliculus to Cortical Area MT. J. Neurosci. *30*, 6342–6354.

Bisley, J.W., and Goldberg, M.E. (2010). Attention, intention, and priority in the parietal lobe. Annu. Rev. Neurosci. *33*, 1–21.

Buffalo, E.A., Fries, P., Landman, R., Liang, H., and Desimone, R. (2010). A backward progression of attentional effects in the ventral stream. Proc. Natl. Acad. Sci. U.S.A. *107*, 361–365.

Chau, B.K.H., Sallet, J., Papageorgiou, G.K., Noonan, M.P., Bell, A.H., Walton, M.E., and Rushworth, M.F.S. (2015). Contrasting Roles for Orbitofrontal Cortex and Amygdala in Credit Assignment and Learning in Macaques. Neuron *87*, 1106–1118.

Chelazzi, L., Perlato, A., Santandrea, E., and Della Libera, C. (2013). Rewards teach visual selective attention. Vision Research *85*, 58–72.

Corbetta, M., and Shulman, G.L. (2002). Control of goal-directed and stimulus-driven attention in the brain. Nat. Rev. Neurosci. *3*, 201–215.

Desimone, R., and Duncan, J. (1995). Neural mechanisms of selective visual attention. Annu. Rev. Neurosci. *18*, 193–222.

Downar, J., Crawley, A.P., Mikulis, D.J., and Davis, K.D. (2000). A multimodal cortical network for the detection of changes in the sensory environment. Nat. Neurosci. *3*, 277–283.

van Ede, F., Chekroud, S.R., Stokes, M.G., and Nobre, A.C. (2018). Decoding the influence of anticipatory states on visual perception in the presence of temporal distractors. Nature Communications *9*, 1449.

Egeth, H.E., and Yantis, S. (1997). VISUAL ATTENTION: Control, Representation, and Time Course. Annu. Rev. Psychol. *48*, 269–297.

Failing, M., and Theeuwes, J. (2018). Selection history: How reward modulates selectivity of visual attention. Psychon Bull Rev *25*, 514–538.

Failing, M.F., and Theeuwes, J. (2014). Exogenous visual orienting by reward. J Vis *14*, 6.

Failing, M.F., and Theeuwes, J. (2015). Nonspatial attentional capture by previously rewarded scene semantics. Visual Cognition *23*, 82–104.
Foxe, J.J., and Simpson, G.V. (2002). Flow of activation from V1 to frontal cortex in humans. Exp Brain Res *142*, 139–150.
Frank, D.W., and Sabatinelli, D. (2012). Stimulus-driven reorienting in the ventral frontoparietal attention network: the role of emotional content. Front Hum Neurosci *6*, 116.
Frankó, E., Seitz, A.R., and Vogels, R. (2010). Dissociable neural effects of long-term stimulus-reward pairing in macaque visual cortex. J Cogn Neurosci *22*, 1425–1439.
Ghazizadeh, A., Griggs, W., Leopold, D.A., and Hikosaka, O. (2018). Temporal-prefrontal cortical network for discrimination of valuable objects in long-term memory. Proc. Natl. Acad. Sci. U.S.A. *115*, E2135–E2144.
Gottlieb, J., and Snyder, L.H. (2010). Spatial and non-spatial functions of the parietal cortex. Curr. Opin. Neurobiol. *20*, 731–740.
Griggs, W.S., Amita, H., Gopal, A., and Hikosaka, O. (2018). Visual Neurons in the Superior Colliculus Discriminate Many Objects by Their Historical Values. Front Neurosci *12*, 396.
Hélie, S., Ell, S.W., and Ashby, F.G. (2015). Learning robust cortico-cortical associations with the basal ganglia: An integrative review. Cortex *64*, 123–135.
Hickey, C., and Peelen, M.V. (2015). Neural Mechanisms of Incentive Salience in Naturalistic Human Vision. Neuron *85*, 512–518.
Hickey, C., and Peelen, M.V. (2017). Reward Selectively Modulates the Lingering Neural Representation of Recently Attended Objects in Natural Scenes. J. Neurosci. *37*, 7297–7304.
Hickey, C., Chelazzi, L., and Theeuwes, J. (2010). Reward Changes Salience in Human Vision via the Anterior Cingulate. J. Neurosci. *30*, 11096–11103.
Hikosaka, O., Kim, H.F., Amita, H., Yasuda, M., Isoda, M., Tachibana, Y., and Yoshida, A. (2018). Direct and indirect pathways for choosing objects and actions. Eur. J. Neurosci.
Hillebrand, A., and Barnes, G.R. (2002). A quantitative assessment of the sensitivity of whole-head MEG to activity in the adult human cortex. Neuroimage *16*, 638–650.
Houk, J.C., and Wise, S.P. (1995). Distributed modular architectures linking basal ganglia, cerebellum, and cerebral cortex: their role in planning and controlling action. Cereb. Cortex *5*, 95–110.
Husain, M., and Nachev, P. (2007). Space and the parietal cortex. Trends in Cognitive Sciences *11*, 30–36.
Itthipuripat, S., Cha, K., Rangsipat, N., and Serences, J.T. (2015). Value-based attentional capture influences context-dependent decision-making. J. Neurophysiol. *114*, 560–569.
Jahfari, S., and Theeuwes, J. (2017). Sensitivity to value-driven attention is predicted by how we learn from value. Psychon Bull Rev *24*, 408–415.
Kahnt, T., Heinzle, J., Park, S.Q., and Haynes, J.-D. (2010). The neural code of reward anticipation in human orbitofrontal cortex. PNAS *107*, 6010–6015.
Kim, H.F., and Hikosaka, O. (2013). Distinct basal ganglia circuits controlling behaviors guided by flexible and stable values. Neuron *79*, 1001–1010.
Kleiner, M., Brainard, D., Pelli, D., Ingling, A., Murray, R., and Broussard, C. (2007). What's new in psychtoolbox-3. Perception. *36*, 1–16.
van Koningsbruggen, M.G., Ficarella, S.C., Battelli, L., and Hickey, C. (2016). Transcranial random-noise stimulation of visual cortex potentiates value-driven attentional capture. Soc Cogn Affect Neurosci *11*, 1481–1488.

Lawrence, M.A. (2016). ez: Easy Analysis and Visualization of Factorial Experiments.
Leathers, M.L., and Olson, C.R. (2017). In monkeys making value-based decisions, amygdala neurons are sensitive to cue value as distinct from cue salience. J. Neurophysiol. *117*, 1499–1511.
Lebreton, M., Jorge, S., Michel, V., Thirion, B., and Pessiglione, M. (2009). An automatic valuation system in the human brain: evidence from functional neuroimaging. Neuron *64*, 431–439.
Ledoit, O., and Wolf, M. (2004). A well-conditioned estimator for large-dimensional covariance matrices. Journal of Multivariate Analysis *88*, 365–411.
LeMessurier, A.M., and Feldman, D.E. (2018). Plasticity of population coding in primary sensory cortex. Current Opinion in Neurobiology *53*, 50–56.
Luck, S.J., Woodman, G.F., and Vogel, E.K. (2000). Event-related potential studies of attention. Trends in Cognitive Sciences *4*, 432–440.
Luque, D., Beesley, T., Morris, R.W., Jack, B.N., Griffiths, O., Whitford, T.J., and Le Pelley, M.E. (2017). Goal-Directed and Habit-Like Modulations of Stimulus Processing during Reinforcement Learning. J. Neurosci. *37*, 3009–3017.
MacLean, M.H., and Giesbrecht, B. (2015a). Neural evidence reveals the rapid effects of reward history on selective attention. Brain Res. *1606*, 86–94.
MacLean, M.H., and Giesbrecht, B. (2015b). Irrelevant reward and selection histories have different influences on task-relevant attentional selection. Atten Percept Psychophys *77*, 1515–1528.
MacLean, M.H., Diaz, G.K., and Giesbrecht, B. (2016). Irrelevant learned reward associations disrupt voluntary spatial attention. Atten Percept Psychophys *78*, 2241–2252.
Marcus, D., Harwell, J., Olsen, T., Hodge, M., Glasser, M., Prior, F., Jenkinson, M., Laumann, T., Curtiss, S., and Van Essen, D. (2011). Informatics and Data Mining Tools and Strategies for the Human Connectome Project. Front. Neuroinform. *5*.
Menon, V., and Uddin, L.Q. (2010). Saliency, switching, attention and control: a network model of insula function. Brain Struct Funct *214*, 655–667.
Merre, P.L., Esmaeili, V., Charrière, E., Galan, K., Salin, P.-A., Petersen, C.C.H., and Crochet, S. (2018). Reward-Based Learning Drives Rapid Sensory Signals in Medial Prefrontal Cortex and Dorsal Hippocampus Necessary for Goal-Directed Behavior. Neuron *97*, 83-91.e5.
Miyashita, Y. (1988). Neuronal correlate of visual associative long-term memory in the primate temporal cortex. Nature *335*, 817–820.
Moore, T., and Zirnsak, M. (2017). Neural Mechanisms of Selective Visual Attention. Annual Review of Psychology *68*, 47–72.
Nolte, G. (2003). The magnetic lead field theorem in the quasi-static approximation and its use for magnetoencephalography forward calculation in realistic volume conductors. Phys. Med. Biol. *48*, 3637.
Oostenveld, R., Fries, P., Maris, E., and Schoffelen, J.-M. (2011). FieldTrip: Open source software for advanced analysis of MEG, EEG, and invasive electrophysiological data. Comput Intell Neurosci *2011*, 156869.
Op de Beeck, H.P., and Baker, C.I. (2010). The Neural Basis of Visual Object Learning. Trends Cogn Sci *14*, 22.
Peck, C.J., and Salzman, C.D. (2014). Amygdala neural activity reflects spatial attention towards stimuli promising reward or threatening punishment. Elife *3*.
Peck, C.J., Jangraw, D.C., Suzuki, M., Efem, R., and Gottlieb, J. (2009). Reward modulates attention independently of action value in posterior parietal cortex. J. Neurosci. *29*, 11182–11191.

Peck, E.L., Peck, C.J., and Salzman, C.D. (2014). Task-dependent spatial selectivity in the primate amygdala. J. Neurosci. *34*, 16220–16233.

Poort, J., Khan, A.G., Pachitariu, M., Nemri, A., Orsolic, I., Krupic, J., Bauza, M., Sahani, M., Keller, G.B., Mrsic-Flogel, T.D., et al. (2015). Learning Enhances Sensory and Multiple Non-sensory Representations in Primary Visual Cortex. Neuron *86*, 1478–1490.

Posner, M.I. (1980). Orienting of attention. Quarterly Journal of Experimental Psychology *32*, 3–25.

Qi, S., Zeng, Q., Ding, C., and Li, H. (2013). Neural correlates of reward-driven attentional capture in visual search. Brain Res. *1532*, 32–43.

Raymond, J.E., and O'Brien, J.L. (2009). Selective visual attention and motivation: the consequences of value learning in an attentional blink task. Psychol Sci *20*, 981–988.

Richards, J.E., Sanchez, C., Phillips-Meek, M., and Xie, W. (2016). A database of age-appropriate average MRI templates. Neuroimage *124*, 1254–1259.

Saalmann, Y.B., and Kastner, S. (2009). Gain control in the visual thalamus during perception and cognition. Curr. Opin. Neurobiol. *19*, 408–414.

Sasikumar, D., Emeric, E., Stuphorn, V., and Connor, C.E. (2018). First-Pass Processing of Value Cues in the Ventral Visual Pathway. Current Biology *28*, 538-548.e3.

Schoups, A., Vogels, R., Qian, N., and Orban, G. (2001). Practising orientation identification improves orientation coding in V1 neurons. Nature *412*, 549–553.

Smith, S.M., and Nichols, T.E. (2009). Threshold-free cluster enhancement: addressing problems of smoothing, threshold dependence and localisation in cluster inference. Neuroimage *44*, 83–98.

Srihasam, K., Vincent, J.L., and Livingstone, M.S. (2014). Novel domain formation reveals proto-architecture in inferotemporal cortex. Nat. Neurosci. *17*, 1776–1783.

Theeuwes, J., and Belopolsky, A.V. (2012). Reward grabs the eye: oculomotor capture by rewarding stimuli. Vision Res. *74*, 80–85.

Todd, T.P., Vurbic, D., and Bouton, M.E. (2014). Behavioral and neurobiological mechanisms of extinction in Pavlovian and instrumental learning. Neurobiology of Learning and Memory *108*, 52–64.

Van Veen, B.D., van Drongelen, W., Yuchtman, M., and Suzuki, A. (1997). Localization of brain electrical activity via linearly constrained minimum variance spatial filtering. IEEE Trans Biomed Eng *44*, 867–880.

Vuilleumier, P. (2015). Affective and motivational control of vision. Current Opinion in Neurology *28*, 29.

Walther, A., Nili, H., Ejaz, N., Alink, A., Kriegeskorte, N., and Diedrichsen, J. (2016). Reliability of dissimilarity measures for multi-voxel pattern analysis. Neuroimage *137*, 188–200.

Wang, L., Yu, H., Hu, J., Theeuwes, J., Gong, X., Xiang, Y., Jiang, C., and Zhou, X. (2015). Reward breaks through center-surround inhibition via anterior insula. Hum Brain Mapp *36*, 5233–5251.

Wimmer, G.E., Li, J.K., Gorgolewski, K.J., and Poldrack, R.A. (2018). Reward learning over weeks versus minutes increases the neural representation of value in the human brain. J. Neurosci. 0075–18.

Winkler, A.M., Ridgway, G.R., Webster, M.A., Smith, S.M., and Nichols, T.E. (2014). Permutation inference for the general linear model. Neuroimage *92*, 381–397.

Wolff, M.J., Ding, J., Myers, N.E., and Stokes, M.G. (2015). Revealing hidden states in visual working memory using electroencephalography. Front Syst Neurosci *9*, 123.

Wolff, M.J., Jochim, J., Akyürek, E.G., and Stokes, M.G. (2017). Dynamic hidden states underlying working-memory-guided behavior. Nat. Neurosci. *20*, 864–871.

Woodman, G.F., and Luck, S.J. (1999). Electrophysiological measurement of rapid shifts of attention during visual search. Nature *400*, 867–869.

Woolrich, M., Hunt, L., Groves, A., and Barnes, G. (2011). MEG Beamforming using Bayesian PCA for Adaptive Data Covariance Matrix Regularisation. Neuroimage *57*, 1466–1479.

Yamamoto, S., Monosov, I.E., Yasuda, M., and Hikosaka, O. (2012). What and where information in the caudate tail guides saccades to visual objects. J. Neurosci. *32*, 11005–11016.

Yamamoto, S., Kim, H.F., and Hikosaka, O. (2013). Reward value-contingent changes of visual responses in the primate caudate tail associated with a visuomotor skill. J. Neurosci. *33*, 11227–11238.

Yasuda, M., and Hikosaka, O. (2015). Functional territories in primate substantia nigra pars reticulata separately signaling stable and flexible values. J. Neurophysiol. *113*, 1681–1696.

Yasuda, M., and Hikosaka, O. (2018). Medial thalamus in the territory of oculomotor basal ganglia represents stable object value. Eur. J. Neurosci.

Zelinsky, G.J., and Bisley, J.W. (2015). The what, where, and why of priority maps and their interactions with visual working memory. Ann. N. Y. Acad. Sci. *1339*, 154–164.